Chapter 24
Discrete Thermomechanics: From Thermal Echo to Ballistic Resonance (A Review)

Ekaterina A. Podolskaya, Anton M. Krivtsov, and Vitaly A. Kuzkin

Abstract We present a review of the results in the field of discrete thermomechanics that have been achieved in the Institute for Problems in Mechanical Engineering RAS over the past decade. The focus is set on the novel approach for analytical description of non-equilibrium thermomechanical processes in crystalline solids. One, two, and three-dimensional perfect crystals with arbitrary harmonic and weakly anharmonic interactions are considered. The discussed topics cover three major areas: transition to thermal equilibrium, ballistic heat transfer, and thermoelasticity. The analysis reveals and elucidates such phenomena as thermal waves, heat flow from "cold" to "hot", the existence of several kinetic temperatures, thermal echo, and ballistic resonance.

Keywords Ballistic heat transport · Ballistic resonance · Transient processes · Thermal waves · Kinetic temperature

24.1 Introduction

One of the topical problems of solid mechanics is the calculation of thermoelastic fields in materials and structures under various external influences. The continuum linear thermoelasticity theory provides an adequate and consistent description of the behavior of materials at the macro level. In particular, the problem of determining the temperature field causing thermoelastic stresses at the macro level is usually successfully solved using the Fourier law. The law describes the diffusive transfer of thermal energy, which is typical for macroscopic systems. However, the recent experiments reported in the works of Zettl [14], Maznev and Huberman [41], Nelson [49], Rogers [101], etc. indicate that at the micro- and nanoscale levels the

E. A. Podolskaya (✉) · A. M. Krivtsov · V. A. Kuzkin
Institute for Problems in Mechanical Engineering RAS, V.O., Bolshoy pr., 61, St. Petersburg 199178, Russia
e-mail: akrivtsov@bk.ru

Peter the Great St. Petersburg Polytechnic University, Polytekhnicheskaya, 29, St. Petersburg 195259, Russia

V. A. Polyanskiy and A. K. Belyaev (eds.), *Mechanics and Control of Solids and Structures*, Advanced Structured Materials 164,
https://doi.org/10.1007/978-3-030-93076-9_24

thermal energy can spread in a wave manner. In particular, it is shown that in many materials, including nanowires, carbon nanotubes, graphene, silicon membranes, etc., significant deviations from the Fourier law are observed. Theoretical investigation of this issue is addressed worldwide by Chen [15], Dhar [18, 19, 50], Gendelman and Savin [26, 27, 104, 105], Hemmer [34], Kosevich [58], Lebowitz [12, 50, 78, 100], Lepri, Livi and Politi [81–83], Lukkarinen [33], Mielke [90], Slepyan [108], Spohn [109], and many other authors. In such context, the development of mechanical models describing the thermoelastic behavior of solids, taking into account the ballistic transfer of thermal energy, becomes relevant. This goal is essential in connection with the development of microprocessor technology and the problem of heat removal from processors. In the Institute for Problems in Mechanical Engineering of the Russian Academy of Sciences (IPME RAS), the comprehensive study in this field was initiated by our research group in the works of Krivtsov [60, 61], followed by a series of papers, for example, [8, 23–25, 62–66, 70–77, 80, 85, 86, 91, 96, 111–113].

Anomalous heat transfer is closely connected with more general problems of non-equilibrium thermomechanical behavior of materials. This topic is considered in the works of Allen [2], Belyaev and Indeitsev [43, 44], Dmitriev [103], Dudnikova [20], Fortov [3, 45], Gavrilov [24, 25], Guzev [32], Ivanova [48], Krivtsov [60, 61, 64], Kukushkin [68, 69], Kuzkin [73, 75], Lurie [87, 88], Muratikov [92], Müller [62, 111], Petrov [45], Prigogine [98], Vilchevskaya [112], etc. At thermal equilibrium, the kinetic energy is usually equally distributed among the degrees of freedom. This fact makes it possible to describe the thermal state of an elementary volume of a material using a single scalar parameter – *kinetic temperature* proportional to the energy of chaotic thermal motion of atoms. Far from thermal equilibrium, the kinetic energies corresponding to the different degrees of freedom can differ significantly. As a result, it is necessary to introduce several temperatures. In particular, it is known that the lattice and electron subsystem temperatures in laser exposed solids may vary [43]. Multiple temperatures are also found in molecular dynamics simulations of shock waves [3, 35] and simulations of heat propagation in polyatomic crystal lattices [74]. It is often necessary to describe the process of energy equilibration, corresponding to different degrees of freedom. To describe this transient process within multicomponent continuum mechanics models, the construction of appropriate constitutive equations is required.

Discrete models of solids can be effectively used to simulate the thermomechanical behavior of materials at the micro- and nanoscale and construct continuum constitutive equations, e.g., referred to in the papers by Abramian et al. [1], Belyaev et al. [97], Dmitriev [7], Fortov [3, 45], Goldstein and Morozov [28], Golovneva et al. [29, 30], Ivanova [46, 47], Korobeynikov [56], Krivtsov [59], Norman [67, 93], Psakhie [99], and other authors. In particular, different variations of the particle method, such as the method of molecular dynamics [2] or the method of movable cellular automata [99], have become widely used.

The main objective of the present work is to provide a review of methods for *analytical* description of thermomechanical processes in crystalline solids that have been developed at IPME RAS over the past few years. After a brief notation outline

in Sect. 24.2, the paper is organized as follows. In Sect. 24.3, the so-called "fast" processes, i.e., energy equilibration and redistribution among the degrees of freedom, are considered. Next, Sect. 24.4 addresses the "slow" process (ballistic heat transfer). The paper is concluded by Sect. 24.5, where the conversion of thermal energy into mechanical energy and vice versa is considered.

24.2 Nomenclature

We use lower-case letters in boldface for vectors, either upper-case letters or Greek letters in boldface for tensors, and italic for scalars. The following notation is used:

- $d = 1, 2, 3$ is the space dimension;
- m and C are the particle mass and bond stiffness; C_1 is the substrate stiffness;
- $\omega_e = \sqrt{C/m}$ is the characteristic frequency, $\tau_e = 2\pi/\omega_e$ is the characteristic period of oscillations, and $c = \omega_e a$ is the characteristic velocity;
- η is damping coefficient, $\widehat{\omega}_e = 1/4\sqrt{16\omega_e^2 - \eta^2}$ is the characteristic frequency for non-conservative problems;
- $\mathbf{r}$ is the position vector of a particle (or a unit cell—see Sects. 24.3.1.3 and 24.4.2);
- $\mathbf{a}_\alpha$ is the vector connecting this particle (or unit cell—see Sects. 24.3.1.3 and 24.4.2) with neighboring particle/cell number α; $a_\alpha \equiv |\mathbf{a}_\alpha|$, $\mathbf{e}_\alpha \equiv \mathbf{a}_\alpha/a_\alpha$;
- $\mathbf{u}(\mathbf{r})$ and $\mathbf{v}(\mathbf{r})$ are the displacement and velocity of a particle (or columns, consisting of components of displacements and velocities of particles from unit cell—see Sects. 24.3.1.3 and 24.4.2);
- $\mathbf{u}_0(\mathbf{r})$ and $\mathbf{v}_0(\mathbf{r})$ are the initial displacement and velocity of a particle (or the respective columns—see Sects. 24.3.1.3 and 24.4.2);
- $\boldsymbol{\xi}(\mathbf{r}_i, \mathbf{r}_j) = \langle \mathbf{u}(\mathbf{r}_i)\mathbf{u}(\mathbf{r}_j) \rangle$ and $\varkappa(\mathbf{r}_i, \mathbf{r}_j) = \langle \mathbf{v}(\mathbf{r}_i)\mathbf{v}(\mathbf{r}_j) \rangle$ are the tensor covariances of displacements and velocities for a pair of particles i and j; brackets $\langle\rangle$ denote the mathematical expectation; $\mathbf{u}(\mathbf{r}_i)\mathbf{u}(\mathbf{r}_j)$ is the tensor product of the respective displacements;
- $\mathbf{D}$ is the tensor difference operator, D is the respective scalar difference operator;
- $\mathbf{K}$, $\mathbf{\Pi}$, and $\mathbf{L}$ are generalized (non-local) kinetic energy, potential energy, and Lagrangian;
- $\mathbf{T}(\mathbf{r})$ is the tensor temperature, and $T \equiv \mathrm{tr}\mathbf{T}/d$ is the kinetic temperature;
- $J_k(\tau)$ is the Bessel function of the first kind;
- $\mathbf{k}$ is the wave vector, $\omega(\mathbf{k})$ is the dispersion relation, and $\mathbf{c} = \mathrm{d}\omega/\mathrm{d}\mathbf{k}$ is the group velocity vector.

24.3 Transient Processes

The solution of problems of thermomechanics for materials in a highly non-equilibrium state is one of the topical questions of solid mechanics. At thermal equilibrium, the kinetic energy is conventionally accepted to be equally distributed

among the degrees of freedom. This fact follows from the equipartition theorem [38, 119]. This theorem allows us to describe the thermal state of the system using a single scalar parameter of kinetic temperature proportional to the energy of chaotic thermal motion of the atoms. As mentioned above, the kinetic energies corresponding to various degrees of freedom can differ significantly far from thermal equilibrium, so in many works several temperatures are introduced [11, 31, 44, 45]. For example, in papers [36, 37, 116] it is shown that the kinetic energies (temperatures) corresponding to the motions of atoms along and across the direction of shock wave propagation can differ almost by a factor of two near its front. In [50, 51] the heat propagation in a diatomic one-dimensional harmonic chain placed between two thermal reservoirs with different temperatures was considered. It was shown that the temperatures of the sublattices in the non-equilibrium stationary state are different. A similar effect observed for unsteady heat transfer is demonstrated in Sect. 24.3.1.1 [74].

In the absence of any external influences, the non-equilibrium system tends to thermal equilibrium. The transition to thermal equilibrium is accompanied by several processes:

- The velocity distribution function tends to Gaussian [20, 34, 52, 78, 109];
- The total energy is redistributed among kinetic and potential forms [2, 52, 108] (also described below following [5, 60, 71]);
- The kinetic energy is redistributed among the degrees of freedom (addressed below following [71, 73]);
- The energy is redistributed among the system's eigenmodes [98].

These processes, except for the last one, occur both in linear (harmonic) and nonlinear systems [2, 20, 52, 60, 71, 78, 109]. In harmonic crystals, the energies of the eigenmodes are constant in time. However, the kinetic temperature field in infinite harmonic crystals tends to become spatially homogeneous and constant in time [34, 72, 109]. Therefore, the concept of thermal equilibrium has been widely applied to harmonic crystals [10, 20, 42, 78, 109, 114].

The transition to thermal equilibrium is considered in many works, and such aspects of this process as the existence of an equilibrium state [78], ergodicity [114], the normalization of the distribution function [10, 20, 52], entropy evolution [42, 111], etc. have been investigated. The present section deals with the behavior of the main experimentally observed value of the kinetic temperature(s), which is proportional to the kinetic energy of chaotic particle motion.

There exist two different approaches to describe the behavior of statistical characteristics in harmonic crystals. One of them is based on the exact solution of the lattice dynamics equations to calculate the kinetic temperature as the mathematical expectation of the kinetic energy [32, 42, 52, 84]. In particular, the pioneering work of Klein and Prigogine [52] considered the transition to thermal equilibrium in an infinite harmonic chain with random initial conditions. Using the exact solution obtained by Schrödinger [106], it was shown that the kinetic and potential energies of the chain oscillate in time and tend to equal equilibrium values [52].

The present section focuses on the other approach, which uses covariances of velocities and covariances of particle motions as the main variables (the covariance

of two centered random variables is the mathematical expectation of their product). In the case of a harmonic crystal, it is possible to obtain a closed system of equations for the covariance in the stationary [50, 82, 100] and non-stationary [60, 83] cases. The solution of this system describes, in particular, the change in kinetic temperature over time. In Sects. 24.3.1.1–24.3.1.3 this idea is used to describe the transition to equilibrium in infinite crystals with monoatomic and polyatomic lattice. In particular, one-dimensional chains [5, 60, 73] and two-dimensional triangular, square, and hexagonal (graphene) lattices [70–73] are considered. Next, in Sects. 24.3.2–24.3.4 several generalizations are introduced, such as damping [23], weak interaction nonlinearity [71, 75], and account for the lattice finiteness [91]. The latter is concluded by the effect of *thermal echo*.

24.3.1 Infinite Harmonic Crystal

We begin with the simplest mathematical model. Consider an infinite simple crystal lattice in the space of dimension d, which consists of identical particles. The particles positions are identified by the vectors in the undeformed state, and the nearest neighbors interact via linearized, or *harmonic*, forces. The Born-von Karman periodic boundary conditions [4] are used.

First, we formulate the *stochastic* problem. The equations of motion[1] take the form of the differential-difference equations, equivalent to the infinite[2] system of second-order ODEs [71]:

$$\begin{aligned} &\dot{\mathbf{v}}(\mathbf{r}) = \mathbf{D}\cdot\mathbf{u}(\mathbf{r}), \qquad \mathbf{D} = \omega_e^2 \sum_{\alpha} \mathbf{e}_\alpha \mathbf{e}_\alpha \Delta_\alpha^2, \\ &\Delta_\alpha^2 \mathbf{u}(\mathbf{r}) = \mathbf{u}(\mathbf{r}+\mathbf{a}_\alpha) - 2\mathbf{u}(\mathbf{r}) + \mathbf{u}(\mathbf{r}-\mathbf{a}_\alpha). \end{aligned} \tag{24.1}$$

The initial conditions are written as

$$\mathbf{u}(\mathbf{r})\Big|_{t=0} = \mathbf{u}_0(\mathbf{r}), \qquad \mathbf{v}(\mathbf{r})\Big|_{t=0} = \mathbf{v}_0(\mathbf{r}), \tag{24.2}$$

where $\mathbf{u}_0(\mathbf{r})$ and $\mathbf{v}_0(\mathbf{r})$ are uncorrelated *random* vectors with zero mean, i.e., $\langle \mathbf{u}_0(\mathbf{r})\rangle = 0$, $\langle \mathbf{v}_0(\mathbf{r})\rangle = 0$.

The solution of the system (24.1)–(24.2) describes the crystal dynamics completely. Moreover, these equations can be solved analytically. However, the description of the thermal processes usually requires only the statistical characteristics, such as covariances of velocities $\varkappa(\mathbf{r}_i, \mathbf{r}_j) = \langle \mathbf{v}(\mathbf{r}_i)\mathbf{v}(\mathbf{r}_j)\rangle$ and displacements $\boldsymbol{\xi}(\mathbf{r}_i, \mathbf{r}_j) = \langle \mathbf{u}(\mathbf{r}_i)\mathbf{u}(\mathbf{r}_j)\rangle$ of particles i and j. Following [71] and the references therein, we write down the *deterministic* system of second-order tensor ODEs:

---

[1] These equations are valid only for the simple, or *monoatomic*, lattices. The general formulae for the *polyatomic* lattices can be found in, e.g., [73], and the results are addressed in Sect. 24.3.1.3.

[2] For infinite crystals.

$$\begin{aligned} \ddot{\boldsymbol{\xi}} &= \mathbf{D}\cdot\boldsymbol{\xi} + \boldsymbol{\xi}\cdot\mathbf{D} + 2\varkappa, \\ \ddot{\varkappa} &= \mathbf{D}\cdot\varkappa + \varkappa\cdot\boldsymbol{\xi} + 2\mathbf{D}\cdot\boldsymbol{\xi}\cdot\mathbf{D}. \end{aligned} \tag{24.3}$$

The system (24.3) yields to a single fourth-order equation which is valid both for $\boldsymbol{\xi}$ and $\varkappa$:

$$\dddot{\varkappa} - 2\left(\mathbf{D}\cdot\ddot{\varkappa} + \ddot{\varkappa}\cdot\mathbf{D}\right) + \mathbf{D}^2\cdot\varkappa - 2\mathbf{D}\cdot\varkappa\cdot\mathbf{D} + \varkappa\cdot\mathbf{D}^2 = 0. \tag{24.4}$$

The respective initial conditions will be discussed below for the particular examples. We note that Eq. (24.4) is also satisfied for harmonic crystals with arbitrary polyatomic lattice [73].

Another useful yet not inevitable assumption is the uniform initial temperature distribution. It can be demonstrated that at the time scale at which the transient processes come out and decay, the change in spatial temperature distribution is negligible (see Sect. 24.4 and the references therein). Then, the covariances depend only on the difference between the particles i and j position vectors. In this case, we can introduce a new variable instead:

$$\left(\mathbf{r}_i, \mathbf{r}_j\right) \longrightarrow \left(\mathbf{r}_i - \mathbf{r}_j\right). \tag{24.5}$$

This assumption leads to the simplification of Eq. (24.4).

Basing on the covariances, we introduce the generalized (or non-local) potential and kinetic energies, and also the generalized Lagrangian [61, 70]

$$\begin{aligned} \boldsymbol{\Pi}(\mathbf{r}_i, \mathbf{r}_j) &= -\frac{m}{4}\left(\mathbf{D}\cdot\boldsymbol{\xi}(\mathbf{r}_i, \mathbf{r}_j) + \boldsymbol{\xi}(\mathbf{r}_i, \mathbf{r}_j)\cdot\mathbf{D}\right), \\ \mathbf{K}(\mathbf{r}_i, \mathbf{r}_j) &= \frac{m}{2}\varkappa(\mathbf{r}_i, \mathbf{r}_j), \qquad \mathbf{L} = \mathbf{K} - \boldsymbol{\Pi}. \end{aligned} \tag{24.6}$$

If $i = j$, the traces of tensors $\mathbf{K}$, $\boldsymbol{\Pi}$, and $\mathbf{L}$ are equal to the respective conventional energies per particle. Note that $\mathbf{K}$, $\boldsymbol{\Pi}$, and $\mathbf{L}$ satisfy Eq. (24.4). As for the initial conditions, the use of the conservation laws helps to eliminate the odd derivatives (see, e.g., [71] for the details).

Next, we define the *tensor temperature* $\mathbf{T}(\mathbf{r})$ [36, 37] and *kinetic temperature* T as

$$\frac{k_B}{2}\mathbf{T}(\mathbf{r}) = \mathbf{K}(\mathbf{r}_i, \mathbf{r}_j)\Big|_{i=j}, \qquad T = \frac{1}{d}\mathrm{tr}\mathbf{T}(\mathbf{r}). \tag{24.7}$$

Here k_B is Boltzmann constant. The kinetic temperature is introduced in such a way that at the equilibrium the equipartition theorem [38] is fulfilled, i.e., kinetic energy per degree of freedom is equal to $k_B T/2$.

In the following sections, we consider several generalizations, including the influence of interaction nonlinearity and finiteness of the system. But before that, let us turn to the examples of harmonic crystals. It is noteworthy that in all examples the numerical and analytical solutions demonstrate an excellent agreement.

24.3.1.1 Hooke's Crystal

We start with the one-dimensional case ($d = 1$). Then all the vector and tensor quantities yield to their scalar equivalents. Consider one of the possible transient processes, i.e., the evolution of the generalized Lagrangian [60]. Taking the aforementioned formulae and also conservation laws into account, we get for the particle n

$$\ddot{L}_n = 4\omega_e^2 \Delta_n^2 L_n, \quad \Delta_n^2 L_n = L_{n+1} - 2L_n + L_{n-1}, \qquad 0 < n < N. \tag{24.8}$$

Here the parameter $N \gg 1$ characterizes the length of the period in Born-von Karman boundary conditions. Assuming that the initial velocities of particles are uncorrelated and the initial displacements are absent, the initial conditions yield to

$$L_n\Big|_{t=0} = E\delta_n, \qquad \dot{L}_n\Big|_{t=0} = 0, \tag{24.9}$$

where E is the initial energy of the instantaneous thermal perturbation, $\delta_n = 1$ for $n = 0$; otherwise $\delta_n = 0$. For $N \to \infty$ the solution yields to

$$L_n(t) = E J_{2n}(4\omega_e t) \approx (-1)^n \frac{E}{\sqrt{2\pi\omega_e t}} \cos\left(4\omega_e t - \frac{\pi}{4}\right) + O\left(t^{-3/2}\right). \tag{24.10}$$

Recall, that if $n = 0$, L_n is equal to the conventional Lagrangian. Hence, the Lagrangian, L, satisfies the differential Bessel equation:

$$\ddot{L} + \frac{1}{t}\dot{L} + 16\omega_e^2 L = 0. \tag{24.11}$$

The oscillations occur with frequency $4\omega_e$, and the amplitude decays as the square root of time (see Fig. 24.1).

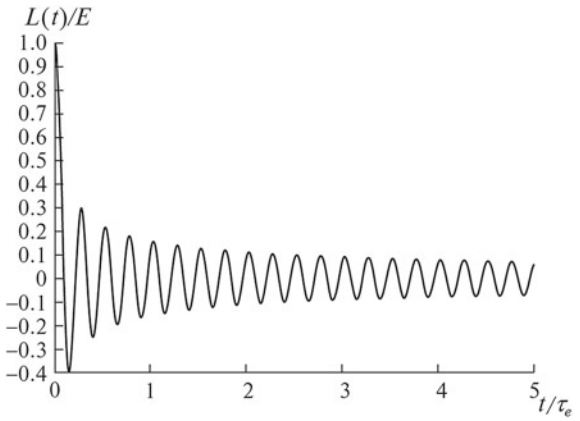

Fig. 24.1 Oscillations of the Lagrangian for the Hooke's crystal [60]

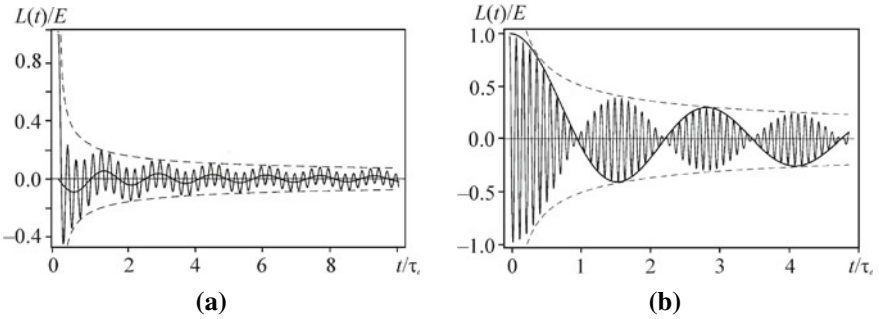

Fig. 24.2 Oscillations of the Lagrangian for (**a**) the soft ($\epsilon = 0.1$) and (**b**) the hard ($\epsilon = 24$) elastic foundations [5]. The dashed lines show the bounding functions

A similar yet essentially different result is obtained for the one-dimensional chain on the elastic foundation [5]. The introduction of the additional stiffness parameter C_1 leads to the modification of Eq. (24.8)

$$\ddot{L}_n = 4\omega_e^2 \left(L_{n+1} - 2(1+\epsilon)L_n + L_{n-1}\right), \qquad \epsilon = \frac{C_1}{C} \tag{24.12}$$

with the same initial conditions (24.9).

If the elastic foundation is soft ($\epsilon < 1$), the solution for the Lagrangian takes the form, which is proved to be valid up to $\epsilon = 1$

$$L = E\left(J_0\left(2\sqrt{4+\epsilon}\omega_e t\right) - \frac{1}{2}\sqrt{\epsilon}J_1\left(2\sqrt{\epsilon}\omega_e t\right)\right). \tag{24.13}$$

The second summand in formula (24.13) gives low-frequency oscillations on which the first high-frequency summand is superimposed (see Fig. 24.2a).

For the hard elastic foundation ($\epsilon > 1$) the solution may be approximately represented as

$$L \approx E J_0(\Omega_2 t)\cos(\Omega_1 t), \quad \Omega_{1,2} = \left(\sqrt{4+\epsilon} \pm \sqrt{\epsilon}\right)\omega_e, \tag{24.14}$$

which leads to the formations of beats: the low-frequency envelope $J_0(\Omega_2 t)$ restricts the wave packet with a high-frequency harmonic signal (see Fig. 24.2b).

24.3.1.2 Two- and Three-Dimensional Crystals

Let us pass over to two-dimensional space ($d = 2$). First, consider the so-called scalar lattices [33, 90, 104]. In this case, a scalar function of a position vector $u(\mathbf{r})$ is used to describe the system motion (24.1), i.e., each particle has only one degree

of freedom, and the temperature (24.7) is also scalar. Note that a one-dimensional chain with nearest neighbor interaction (see Sect. 24.3.1.1) is also a scalar lattice.

The exact solution for the kinetic temperature is given by [72]

$$T = \frac{T_0}{2}\left[1 + \int_{\mathbf{k}} \cos\left(2\omega(\mathbf{k})t\right)\mathrm{d}\mathbf{k}\right], \tag{24.15}$$

where the integration is carried out with respect to components of the wave vector $\mathbf{k}$; $\int_{\mathbf{k}} \mathrm{d}\mathbf{k} = 1$. Here another important quantity is introduced: the dispersion relation $\omega(\mathbf{k})$ which is obtained from lattice dynamics Eqs. (24.1).

In 2D, the first example to be considered is the out-of-plane vibrations of square lattice [72]. In harmonic approximation, in-plane and out-of-plane vibrations of the lattice are independent. The lattice is prestrained; otherwise the oscillations would be essentially nonlinear. The kinetic energy oscillations decay, and the characteristic time of this process is of the order of several characteristic periods τ_e. The rate of decay is proportional to $1/t$ in contrast to the one-dimensional problem for which it decays as $1/\sqrt{t}$. The characteristic frequencies for both one-dimensional and two-dimensional scalar lattices are calculated in [55].

The next step is to consider in-plane vibrations of the square and triangular lattices. In this case, each particle has two degrees of freedom, and the temperature tensor (24.7) has two eigenvalues. The analytical solution of the respective equations [70, 71] clearly demonstrates that, in general, $\mathbf{T}$ is not isotropic, and the velocity covariance for neighboring particles $\varkappa(\mathbf{r}_i, \mathbf{r}_j)$ is not equal to zero, i.e., particles' velocities are not statistically independent (see Fig. 24.3). Thus, we capture another transient process: *temperature redistribution among the degrees of freedom*.[3] The characteristic frequencies for this problem are calculated in [113].

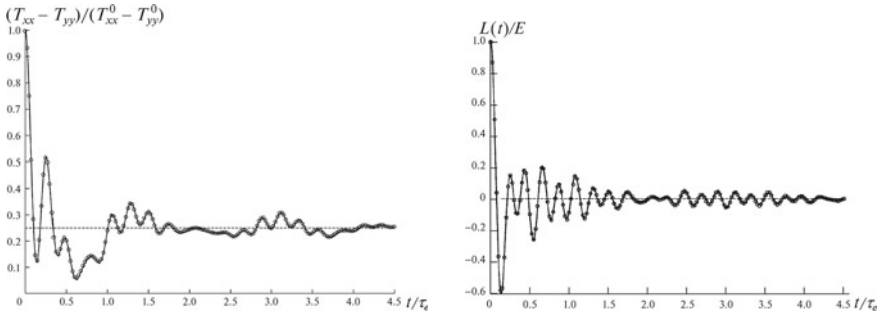

(a) **(b)**

Fig. 24.3 Two transient processes associated with triangular lattice in-plane motion: (**a**) temperature redistribution among spatial directions and (**b**) oscillations of the Lagrangian [70]

[3] The rate of decay for triangular lattice is again proportional to $1/t$, whereas for square lattice it decreases as $1/\sqrt{t}$. Moreover, the spatial redistribution effect doesn't appear in the square lattice.

The above derivations are valid not only for $d = 2$ but also for $d = 3$. The results similar to those shown in Fig. 24.3 are obtained in [75] for the face-centered cubic lattice.

24.3.1.3 Polyatomic Crystals

Next, we consider the effects observed only in polyatomic lattices [73].

The unit cells of polyatomic lattices are identified by their position vectors $\mathbf{r}$, and each unit cell has M degrees of freedom, corresponding to components of particles displacements. Hence, instead of tensor temperature (24.7), we introduce the *temperature matrix* $\boldsymbol{T}(\mathbf{r})$ [73, 74]. Its components are given by

$$T_{kn} = \frac{1}{k_B}\sqrt{m_k m_n}\langle v_k v_n \rangle, \tag{24.16}$$

where m_k and v_k are the masses and velocities corresponding to the kth degree of freedom. Temperature matrix is related to the *kinetic temperature* T as

$$T = \frac{1}{M}\sum_{k=1}^{M} T_{kk}. \tag{24.17}$$

The explicit problem statement and derivation of the formulae that describe the time evolution of the temperature matrix are given in [73]. Here we restrict ourselves by the graphic results for one-dimensional lattice with alternating masses and stiffnesses (Fig. 24.4) and for the out-of-plane vibrations of graphene (Fig. 24.5). The transient processes associated with in-plane vibrations of graphene are considered in [8].

Figure 24.4a shows that in both cases the difference between temperatures tends to the value $0.3(T_{11}^0 - T_{22}^0)$, but the shape of the curves differs. Therefore, the process of redistribution of temperature between sublattices depends on difference in the initial temperatures of the sublattices. Figure 24.4b demonstrates that for any given mass ratio, the difference between temperatures decreases with decreasing ratio of stiffnesses and tends to a limiting value corresponding to the case when this ratio tends to zero.

As for the graphene, Fig. 24.5 shows beats of difference between temperatures of sublattices. The amplitude of beats decays in time as $1/t$, so at large times, temperatures of sublattices in graphene equilibrate.

Finally, we note that the equilibrium values of kinetic temperatures in harmonic polyatomic lattices are generally different and depend on the initial value of the temperature matrix. In paper [73], the formula relating equilibrium values of kinetic temperatures with initial conditions is derived. The formula is referred to as the *non-equipartition theorem*. The theorem shows, in particular, that the kinetic temperatures

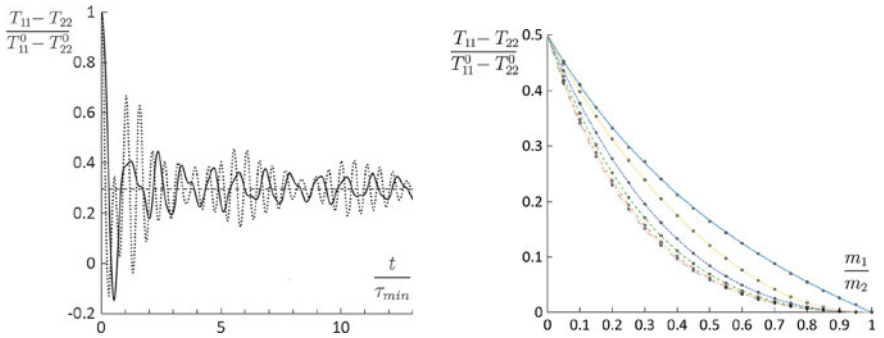

(a) **(b)**

Fig. 24.4 (**a**) Difference between temperatures of sublattices for $T_{11}^0 \neq 0$, $T_{22}^0 = 0$ (solid line) and $T_{11}^0 = 0$, $T_{22}^0 \neq 0$ (dotted line). (**b**) Difference between equilibrium temperatures of sublattices for a diatomic chain with the ratio of stiffnesses equal to 1 (solid line), 1/2 (dotted line), 1/4 (short dashed line), 1/8 (dashed line), 1/16 (dash-dotted line), and 1/32 (dash-double dotted line) [73]

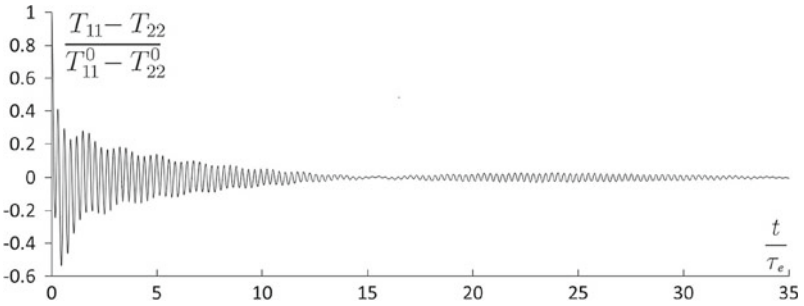

Fig. 24.5 Redistribution of kinetic temperatures among sublattices in graphene [73]

are equal at thermal equilibrium if their initial values are also equal. If initially the kinetic temperatures are different then they are usually different at equilibrium, except for some lattices.

24.3.2 The Influence of Finiteness: Thermal Echo

The account for the finiteness of the one-dimensional harmonic crystal gives rise to more phenomena and effects [91].

The infinite model predicts that the generalized energy oscillations are described by Bessel functions (24.10), and only zero-order Bessel function describes the conventional energies. In contrast, if the crystal consists of a finite number of particles, at a certain time, the amplitude decay, prescribed by the Bessel function, is replaced by a sharp short-term growth which reoccurs periodically. This phenomenon is referred

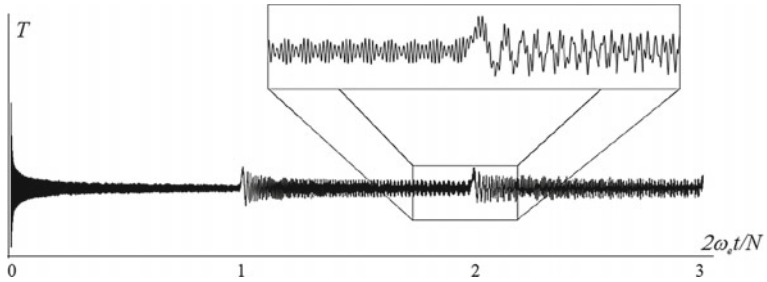

Fig. 24.6 Oscillations of temperature T in the finite Hooke's crystal [91]

to as *thermal echo*, and the sequence of its realizations is described by a series of the Bessel functions of multiple orders. Moreover, a superposition of the temperature oscillations generated by the sequential thermal echoes results in temperature beats with each subsequent thermal echo complicating their shape (see callout in Fig. 24.6).

The solution for, e.g., temperature yields to

$$\begin{aligned} T &= T_E + \frac{\delta T}{2} J_0(4\omega_e t) + \delta T \sum_{p=1}^{p=\infty} J_{2pN}(4\omega_e t), \\ T_E &= \frac{\Delta T}{2}\left(1 - \frac{1}{N-1}\right), \qquad \delta T = \Delta T\left(1 + \frac{1}{N-1}\right). \end{aligned} \tag{24.18}$$

Here T_E is the so-called equilibrium temperature, ΔT is the temperature jump proportional to the initial energy of the instantaneous thermal perturbation E, and N is the number of particles.

Next, it can be shown that in the thermodynamic limit any thermal echo is described by the Airy function; thus formula (24.18) can be rewritten as

$$T = T_E + \frac{\delta T}{2} J_0(4\omega_e t) + \delta T \sum_{p=1}^{p=\infty} \frac{1}{\sqrt[3]{pN}} \mathrm{Ai}\left(\frac{2pN - 4\omega_e t}{\sqrt[3]{pN}}\right). \tag{24.19}$$

So for sufficiently large N any thermal echo is shaped as an Airy function. Hence, the time, when echo p occurs, its relative "height" and "width" are estimated by

$$t_p \simeq \frac{1}{4\omega_e}\left(2pN + \sqrt[3]{pN}\right), \quad h_p \simeq \sqrt{\pi} A_1 \sqrt[6]{pN}, \quad w_p \sim \sqrt[3]{pN}, \tag{24.20}$$

where $A_1 \approx 0.53$ is the first local maximum of Airy function.

The analysis demonstrates that the maximum temperature increase caused by the thermal echo decreases as $\sqrt[3]{pN}$, and the duration of the thermal echo w_p increases with the same rate. Moreover, the amplitude of the temperature oscillations decreases as $1/\sqrt{t}$ between any two echoes. What is more the larger the crystal is, the more

noticeable become the temperature peaks h_p in comparison with the residual oscillations.

24.3.3 The Influence of Dissipation on the Transition to Thermal Equilibrium

In this section, we consider the problem of thermal equilibration in a one-dimensional *damped* harmonic crystal [23].

The problem statement remains almost the same as in Sect. 24.3.1.1. The differential-difference operator, acting on, e.g., generalized Lagrangian, takes the form

$$\frac{\partial^2}{\partial t^2} + 2\eta\frac{\partial}{\partial t} - 4\omega_e^2\Delta_n^2, \tag{24.21}$$

which yields to (24.8) if $\eta = 0$. The characteristic frequency for this equation is $\widehat{\omega}_e = 1/4\sqrt{16\omega_e^2 - \eta^2}$. Unlike the conservative case, the solutions of this kind of equations cannot be evaluated in closed form, so only the asymptotics are estimated.

Omitting a thorough analysis given in [23], we write out the asymptotics for conventional Lagrangian L_0, which would be determined by a waning cosine (24.10) if there was no damping:

$$\begin{aligned}
L &= L^{(1)} + O\left(t^{-7/2}\right) + L^{(2)} + O\left(\frac{e^{-\eta t}}{t}\right),\\
L^{(1)} &= E\left(-\frac{t^{-3/2}}{8\sqrt{2\pi\eta}\omega_e} - \frac{t^{-5/2}\left(3\eta^2 + 12\omega_e^2\right)\sqrt{2}}{512\sqrt{\pi}\eta^{3/2}\omega_e^3}\right),\\
L^{(2)} &= E\frac{e^{-\eta t}}{2\omega_e\sqrt{2\pi t}}\left(2\sqrt{\widehat{\omega}_e}\cos\left(4\widehat{\omega}_e t - \frac{\pi}{4}\right) - \frac{\eta}{2\sqrt{\widehat{\omega}_e}}\sin\left(4\widehat{\omega}_e t - \frac{\pi}{4}\right)\right).
\end{aligned} \tag{24.22}$$

Similar representations can be obtained for the rest of generalized energies. In a particular case of conservative system, the summands with superscript "(1)" disappear, because the integration is carried out over the zero-length interval. In the case of high damping $\eta \geq 4\omega_e$ the summands with superscript "(2)" vanish for the same reason.

If $\eta/\omega_e < 1$ the transient process goes in two phases. Firstly, the kinetic and potential energies oscillate approaching the asymptote $Ee^{-\eta t}/2$, whereas the Lagrangian oscillates tending to zero; their amplitudes decay as the square root of time multiplied by the respective exponent. Secondly, at very large times, the principal term of the asymptotic expansion for the kinetic energy (and, consequently, temperature) becomes proportional to $t^{-5/2}$, whereas the rest of the energies decay as $t^{-3/2}$. In the limiting case of zero dissipation this surprising second phase disappears.

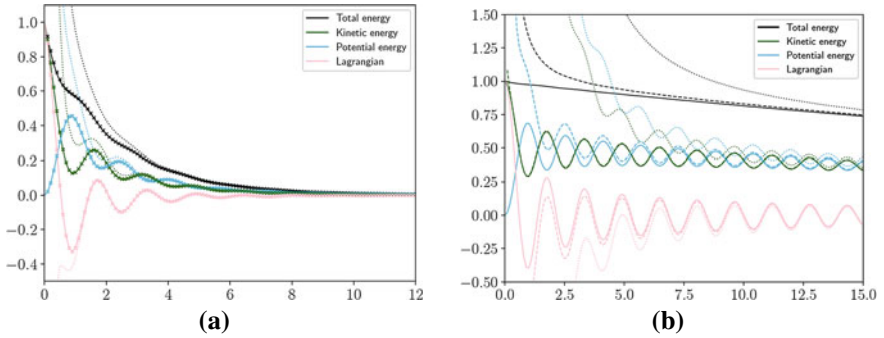

Fig. 24.7 The ratios of generalized energies to the initial value E versus dimensionless time $\omega_e t$ for (**a**) $\eta/\omega_e = 0.5$ and (**b**) $\eta/\omega_e = 0.02$: analytical solutions (solid lines), numerical solutions (crosses), asymptotic solutions (dotted lines), and approximate asymptotic solutions without power-decaying terms (dashed lines; only on the right-hand side) [23]

Note that if the damping is small, i.e., $\eta/\omega_e \ll 1$ the asymptotic formulae give wrong results at finite but not very large times (see Fig. 24.7b), so the valid approximation may be reached and the summands with superscript "(1)" are omitted.

24.3.4 The Influence of Nonlinearity on Transient Thermal Processes

In this example we present the *computational* results of the influence of a weak nonlinearity on the two transient thermal processes described above: (i) equilibration of kinetic and potential energies and (ii) redistribution of the kinetic energy among spatial directions. The account for the process (ii) is possible for both $d = 2$ [71] and $d = 3$ [75].

Let the particles interact via the Lennard-Jones potential:

$$\Pi(r) = \varepsilon \left[\left(\frac{a}{r}\right)^{12} - 2\left(\frac{a}{r}\right)^{6} \right], \tag{24.23}$$

where ε is the bond energy, and a is the equilibrium distance. In order to quantify the influence of nonlinearity, the dissociation velocity $v_d = \sqrt{2\varepsilon/m}$ is introduced. In the simulation the initial velocities are randomly distributed in a circle with radius v_0.

Figure 24.8 shows the results for both transient processes in the triangular lattice. The curve (1) corresponds to $v_0/v_d = 0.05$, (2) is $v_0/v_d = 0.25$, (3) is $v_0/v_d = 0.5$, (4) is analytical solution for harmonic triangular lattice, and (5) is numerical solution of lattice dynamics equations. It is seen that nonlinearity increases the rate of equilibration of the system.

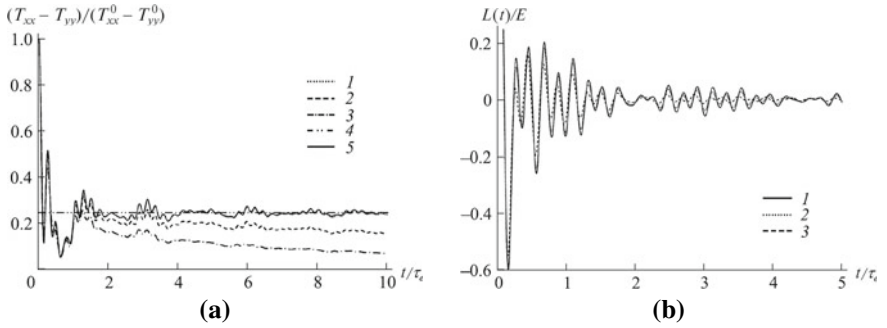

Fig. 24.8 Two transient effects in triangular lattice with Lennard-Jones interaction: (**a**) redistribution of temperature among spatial directions and (**b**) oscillations of the Lagrangian [71]

The additional analysis for FCC lattice [75] has shown that the thermal equilibration has two distinct time scales: the period of atomic vibrations τ_e and anharmonic τ_a, which depends on the initial temperature T_0. These two scales are connected empirically by

$$\frac{\tau_e}{\tau_a} \approx \frac{k_B T_0}{\varepsilon} + 1.496 \left(\frac{k_B T_0}{\varepsilon} \right)^2 - 0.469 \left(\frac{k_B T_0}{\varepsilon} \right)^3 . \tag{24.24}$$

At low temperatures $T_0 < 0.05\varepsilon / k_B$ the second time scale τ_a is almost inversely proportional to the initial temperature.

As far as the first time scale is concerned, the approach to equilibrium is accompanied by decaying high-frequency oscillations of the temperatures at times or order of several τ_e. These oscillations are caused by both transient processes, i.e., equilibration of kinetic and potential energies and redistribution of the kinetic energy among spatial directions.

At time scale τ_a, the difference of the kinetic temperatures deviates from the equilibrium value, predicted by the harmonic approximation, and monotonically tends to zero (see Fig. 24.8).

Thus, in anharmonic crystals thermal equilibration at different temperatures differs only by a time scaling. These results suggest, in particular, that, in the weakly anharmonic case, the characteristic time scales of relaxation and heat transfer may be of the same order; therefore, there may be some mutual influence between these processes.

24.4 Heat Transfer

There are several approaches to the description of heat transfer. In continuum theories, the constitutive equations are usually introduced as part of the phenomenological

approach. In particular, one of the phenomenological equations describing the wave properties of heat propagation is the Maxwell–Cattaneo–Vernotte equation [13, 115]. This equation, unlike the Fourier heat conduction equation, gives a finite speed of heat propagation. However, it still relies on the concept of the thermal conductivity coefficient, which is not a parameter of the material at the micro level. For example, it has been shown that in many materials, including nanowires [39], nanotubes [14], graphene [6, 118], silicone membranes [49], and others, the thermal conductivity depends significantly on the length of the sample on which measurements were carried out. In addition, the Maxwell–Cattaneo–Vernotte equation predicts an exponential decay of thermal perturbations, while in the ballistic regime these perturbations decay according to the power law [61, 74].

Another approach to describing heat propagation at the nanoscale is to use the kinetic Boltzmann equation [94]. This equation is usually simplified using a number of approximations for the collision term, in particular, by introducing relaxation times [9, 53]. This allows the Boltzmann equation to be solved numerically [40, 102], as well as obtaining heat propagation equations [15, 54]. In both cases, additional assumptions are often introduced [107]. In particular, the contribution of optical oscillations to heat transport is often neglected. Comprehensive literature reviews on the use of the Boltzmann equation to describe heat propagation can be found, for example, in [81, 107]. The link between the descriptions based on lattice dynamics and kinetic theory is discussed in [77, 110]. In the present section, the formulae for the heat transfer are derived either from the covariance dynamics equations or from the exact solution of the dynamics equations. This approach makes it possible to take into account all the important features of a discrete system that affect the heat propagation, in particular, to estimate the contribution of the different branches of the dispersion relation.

The analysis of heat transfer in discrete systems is usually carried out in the so-called stationary non-equilibrium state [81, 100]. In this case, the discrete system is placed between two thermostats with different temperatures. The effective heat transfer coefficient of the system is calculated for the known temperature difference, the distance between the thermostats, and the estimated heat flux. This formulation of the problem is widely used both in analytical studies [82, 100] and in computer simulations [19, 50, 81] of heat propagation. A detailed review of the results obtained in the stationary formulation is given, for example, in [18, 81]. Calculation of the effective thermal conductivity coefficient as a function of the sample length makes it possible to determine the conditions under which the ballistic, anomalous, or diffusive mode of heat propagation is realized. In the first case, the heat transfer coefficient increases linearly with length; in the second case it increases nonlinearly; and in the third case it does not depend on length at all. However, the stationary formulation does not allow determining the heat transfer law. Moreover, the results obtained in the stationary formulation may significantly depend on the choice of the thermostat [50]. Therefore, in this paper, we consider the non-stationary formulation of the energy transfer problem.

One of the problems in the study of non-stationary thermal energy transfer is to determine how the initial field of kinetic energy changes in time and space. The

initial field can be set, for example, by giving random initial velocities to particles. In this case, the use of a thermostat is not required. In the literature, such problems are usually solved numerically using, for example, the molecular dynamics method [27, 58, 79, 95]. This method makes it possible to use realistic interaction potentials and to consider the influence of nonlinearity, defects, interfaces, and other features of the real system, which are difficult to take into account analytically. However, in spite of the enormous possibilities of numerical methods, some questions are still easier to address analytically. In particular, for crystals with several branches of the dispersion relation, it is difficult to separate the contribution of different branches to the heat transfer in numerical simulations.

In this section, we continue to use an infinite harmonic crystal as the main model of a crystal. In this model, harmonic waves do not interact with each other, so the heat transfer is purely ballistic. The influence of dissipation and energy supply is regarded in Sect. 24.4.1.2. Once again, note that in all examples the numerical and analytical solutions demonstrate an excellent agreement.

24.4.1 Scalar Lattices

Let us continue the analysis of Eq. (24.4). In contrast to the previous assumption (24.5), here we carry out continualization with respect to spatial variable $\mathbf{r}$ [61, 72], where the following change of variables is employed:

$$\left(\mathbf{r}_i, \mathbf{r}_j\right) \longrightarrow \left(\mathbf{r}, \mathbf{r}_i - \mathbf{r}_j\right), \qquad \mathbf{r} = \frac{\mathbf{r}_i + \mathbf{r}_j}{2}. \tag{24.25}$$

Next, we assume that the covariances are slowly changing functions of $\mathbf{r}$ at distances of order of a_α, then the difference operator can be approximated. Moreover, for the considered type of lattices, all the covariances become scalars (see Sect. 24.3.1.2), so Eq. (24.4) yields to [72]

$$\dddot{\varkappa} - 4D\ddot{\varkappa} + 4(\mathbf{R}\cdot\nabla)^2\varkappa = 0, \tag{24.26}$$

where ∇ is Del operator and the difference operators D and $\mathbf{R}$ are calculated basing on the definition (24.1).

The initial conditions take the form

$$\varkappa = \frac{k_B}{m}T_0(\mathbf{r})\delta(\mathbf{r}_i - \mathbf{r}_j), \quad \dot{\varkappa} = 0, \quad \ddot{\varkappa} = \frac{2k_B}{m}T_0(\mathbf{r})D\delta(\mathbf{r}_i - \mathbf{r}_j), \quad \dddot{\varkappa} = 0, \tag{24.27}$$

where $\delta(\mathbf{r}_i - \mathbf{r}_j)$ is equal to 1 for $i = j$, and vanishes otherwise.

The use of discrete Fourier transform with respect to the wave vector $\mathbf{k}$ allows to obtain the solution in the following form:

$$T = T_F + T_S, \tag{24.28}$$

where T_F is determined by formula (24.15), and it is responsible for transient processes (see Sect. 24.3.1.2). The second summand T_S describes the large-time behavior, and it is equal to

$$T_S = \frac{1}{2}\int_{\mathbf{k}} T_0\big(\mathbf{r} + \mathbf{c}(\mathbf{k})t\big)\mathrm{d}\mathbf{k}, \tag{24.29}$$

where $\mathbf{c}(\mathbf{k}) = \mathrm{d}\omega/\mathrm{d}\mathbf{k}$ is the group velocity.

Thus, formulae (24.15), (24.28), (24.29) fully describe the behavior of the kinetic temperature at both short and large times. They show, in particular, that at large times the temperature field is represented as the superposition of waves traveling with group velocities $\mathbf{c}(\mathbf{k})$.

24.4.1.1 Hooke's Crystal

As discussed before in Sect. 24.3.1.2, one-dimensional lattice is a particular case of scalar lattices, so the formula (24.29) is applicable for this case.

The solution for an infinite Hooke's crystal is given by [61, 64]

$$T(t,x) = \frac{1}{\pi}\int_{-1}^{1}\frac{T_0(x-cts)}{\sqrt{1-s^2}}\mathrm{d}s = \frac{1}{\pi}\int_0^{\pi} T_0(x + ct\cos\varphi)\mathrm{d}\varphi. \tag{24.30}$$

This solution is analyzed in [111] for two examples of the localized ($-l \le x \le l$) initial temperature distribution and compared with the classical heat conduction results. The comparison for the rectangular initial perturbation is shown in Fig. 24.9. The ballistic solution has two strongly pronounced peaks traveling in the positive and negative directions with speed c, whereas the classical solution demonstrates the exponential decay of the single peak in the center.

In [65] the asymptotics for the heat wave described by the ballistic heat transfer Eq. (24.30) is analyzed for several examples of the initial temperature distribution localized in space. The solution in the vicinity of wavefront takes the simple form

$$T\left(t, \frac{x-ct}{l}\right) = \frac{\sqrt{2l}}{\pi\sqrt{ct}}\begin{cases}\displaystyle\int_0^{\sqrt{1-(x-ct)/l}} T_0\left(\frac{x-ct}{l} + p^2\right)\mathrm{d}p, & -l \le x-ct \le l\\ \displaystyle\int_{\sqrt{-1-(x-ct)/l}}^{\sqrt{1-(x-ct)/l}} T_0\left(\frac{x-ct}{l} + p^2\right)\mathrm{d}p, & x-ct \le -l\end{cases} \tag{24.31}$$

This formula shows that the main part of the wave is located in a space region of the same size as the initial localization zone. The thermal wave shrinks vertically as

the square root of time, whereas in the horizontal direction its shape, characterized by the integral, remains unchanged. In addition, it can be demonstrated that during the wave evolution, the wavefront smoothes, e.g., for a power-law dependence, its degree increases by 1/2.

24.4.1.2 Modifications of the One-Dimensional Crystal Model

The effect of the *elastic foundation* on the ballistic heat transfer is discussed in [66], namely, it is shown that in this case the rate of heat transfer is lower than that in the crystal without substrate.

The influence of *damping* and *energy supply* is taken into account in [24]. The respective temperature profiles are obtained analytically and analyzed, e.g. it is shown that the steady-state kinetic temperature distribution caused by a point source of constant intensity is described by the Macdonald function of zero order.

Another modification is the account for the *interaction with the second neighbors* on the crystal lattice [85, 86]. It is shown that the initial thermal perturbation evolves into two consecutive thermal waves propagating with finite and essentially different velocities (see Fig. 24.10a). The velocity of the first front corresponds to the maximum group velocity of the discrete crystalline model. The velocity of the second front is determined by the second group velocity extremum, which arises at a certain ratio between the stiffnesses of the first and second neighbor interaction in the lattice.

To conclude this section, we move away from the scalar lattices concept and mention the generalization of formula (24.29) for the case of one-dimensional crystal with alternating masses or stiffnesses [74, 86, 96] (an arbitrary polyatomic lattice in considered in Sect. 24.4.2):

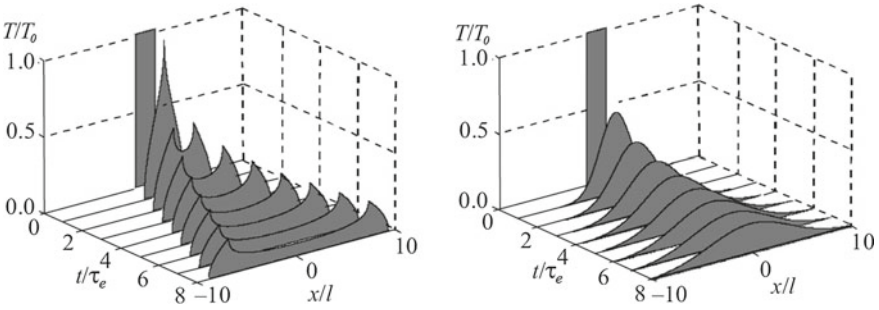

Fig. 24.9 Evolution of the solutions for a rectangular initial perturbation: (**a**) ballistic and (**b**) Fourier heat transfer [111]

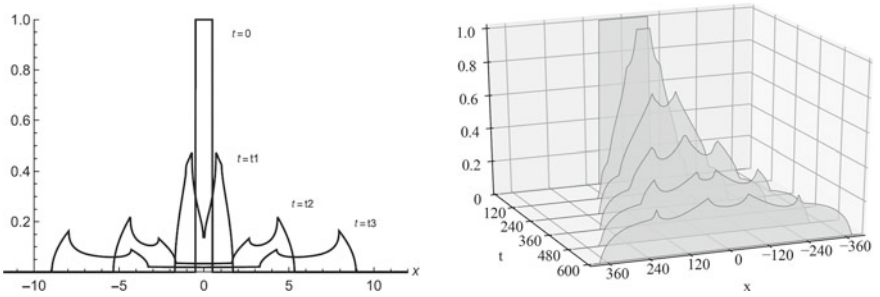

Fig. 24.10 Evolution of the solutions for a rectangular initial perturbation: (**a**) with regard for the second neighbor interaction [85] and (**b**) with alternating masses/stiffnesses [96] (for certain parameters)

$$T_S = \frac{1}{2M} \sum_{j=1}^{M} \int_{\mathbf{k}} T_0\big(x + c_j(k)t\big)\mathrm{d}\mathbf{k}, \tag{24.32}$$

where M is the number of degrees of freedom in the unit cell, and c_j are the respective group velocities ($j = 1 \ldots M$). Formula (24.32) is valid for all one-dimensional harmonic crystals with arbitrary M. In paper [86] it is applied to the diatomic chain. An analytical approach, that allows to identify the thermal wavefront intensity, is proposed. It is demonstrated that, for any ratios between the masses/stiffnesses, the initial thermal perturbation propagates as two successive thermal fronts having finite speeds and repeating the shape of the initial perturbation (see Fig. 24.10b). The speed of the first front corresponds to the acoustic branch of the dispersion relation, and the speed of the second front corresponds to the optical one. In the case when the particle masses differ slightly, the intensity coefficient of the acoustic front is maximum, and the optic front decays, continuing to move at non-zero speed.

24.4.1.3 Two-Dimensional Crystal

The analytical solution of the planar heat transport problem for the stretched square lattice is given in [72].

Figure 24.11a clearly shows two thermal waves traveling in the opposite directions. The peaks of the temperature distribution move with constant speed. Figure 24.11b demonstrates how the heat flows from "cold" (center) to "hot" (peaks).

The influence of the dissipation and heat supply is discussed in [25]. The differential-difference equation describing non-stationary heat propagation in the lattice and the analytical formula in the integral form describing the steady-state kinetic temperature distribution in the lattice caused by a point heat source of a constant intensity are derived.

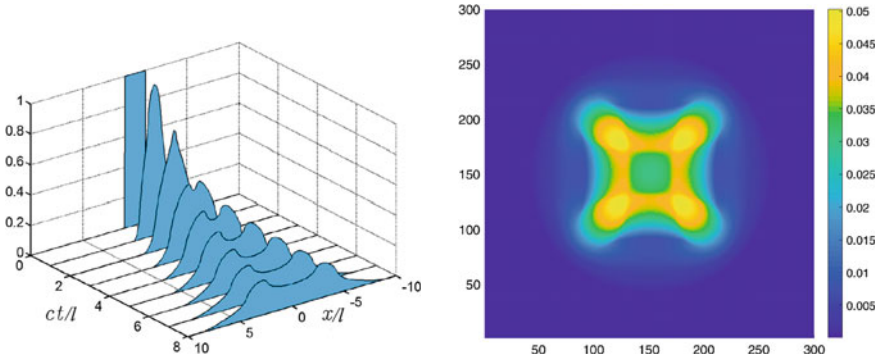

(a) **(b)**

Fig. 24.11 Scalar square lattice [72]: (**a**) evolution of rectangular initial temperature distribution and (**b**) evolution of a circular initial temperature distribution (initial temperature is uniform inside a circle with radius $20a$, and the scale is normalized to the initial temperature value at the center)

24.4.2 Polyatomic Lattices

This section is concluded by the results on heat transfer in polyatomic lattices. The explicit problem statement and respective derivation are given in [74]. We write out the main result, i.e., the approximate formula for the *temperature matrix*:

$$\begin{aligned}
&\boldsymbol{T} = \boldsymbol{T}_F + \boldsymbol{T}_S, \qquad \boldsymbol{T}_F \approx \int_{\mathbf{k}} \boldsymbol{P}\widetilde{\boldsymbol{T}}_F \boldsymbol{P}^{*\mathrm{T}} \mathrm{d}\mathbf{k}, \quad \boldsymbol{T}_S \approx \int_{\mathbf{k}} \boldsymbol{P}\widetilde{\boldsymbol{T}}_S \boldsymbol{P}^{*\mathrm{T}} \mathrm{d}\mathbf{k}, \\
&\left\{\widetilde{\boldsymbol{T}}_F\right\}_{ij} = \frac{1}{2}\left\{\boldsymbol{P}^{*\mathrm{T}}\boldsymbol{T}_0(\mathbf{r})\boldsymbol{P}\right\}_{ij}\left[\cos\left(\left(\omega_i + \omega_j\right)t\right) + \left(1 - \delta_{ij}\right)\cos\left(\left(\omega_i - \omega_j\right)t\right)\right], \\
&\left\{\widetilde{\boldsymbol{T}}_S\right\}_{ij} = \frac{1}{4}\left\{\boldsymbol{P}^{*\mathrm{T}}\Big(\boldsymbol{T}_0\big(\mathbf{r} + \mathbf{c}_j t\big) + \boldsymbol{T}_0\big(\mathbf{r} - \mathbf{c}_j t\big)\Big)\boldsymbol{P}\right\}_{jj}\delta_{ij},
\end{aligned} \tag{24.33}$$

Here $\boldsymbol{P} = \boldsymbol{P}(\mathbf{k})$ is the polarization matrix which consists of normalized eigenvectors of the lattice dynamic matrix, $\mathbf{c}_j(\mathbf{k})$ is the group velocity vector which corresponds to the jth branch of dispersion relation $\omega_j(\mathbf{k})$, and $\boldsymbol{T}_0(\mathbf{r})$ is the initial temperature matrix of the unit cell.

The first term, $\boldsymbol{T}_F$, in formula (24.33) describes short-time behavior of the temperature matrix (fast process). At short times, the temperature matrix oscillates. The oscillations are caused by redistribution of energy among kinetic and potential forms and redistribution of energy among degrees of freedom of the unit cell. These oscillations at different spatial points are independent. At large time scale $\boldsymbol{T}_F$ tends to zero. The second term, $\boldsymbol{T}_S$, in formula (24.33) describes the large time behavior of the temperature matrix (slow process). At large time scale, changes in the temperature profile are caused by ballistic heat transport. The temperature matrix is represented as a superposition of waves traveling with group velocities. Shapes of the waves are

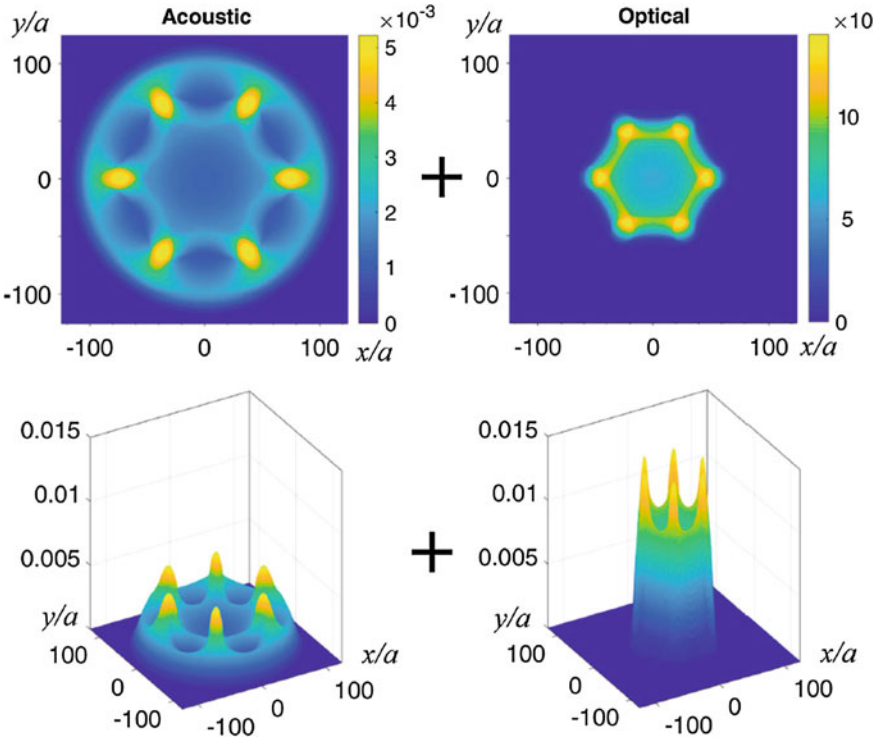

Fig. 24.12 Contributions of acoustic (left) and optical (right) vibrations to temperature profile in graphene at large time. The initial temperature is distributed inside a circle with a radius $10a$. Plus signs mean that the resulting temperature profile is equal to a sum of acoustic and optical contributions. Color bars show the ratio between current and initial temperatures [74]

determined by initial temperature profile $\boldsymbol{T}_0$. Note that according to formula (24.33), accurate description of ballistic heat transport requires knowledge of the dispersion relation and corresponding group velocities. It is noteworthy that the local values of temperatures, corresponding to the degrees of freedom of the unit cell, at large times are generally neither equal to each other nor equal to their equilibrium values (temperature matrix is generally not isotropic). Therefore, the thermal state of unit cells reached by thermal waves is strongly non-equilibrium. In [74] this fact is demonstrated for the chain with alternating masses.

As in Sect. 24.3.1.3, we again restrict ourselves by the graphic results for one-dimensional lattice with alternating masses and stiffnesses (Fig. 24.10) and for the out-of-plane vibrations of graphene (Fig. 24.12).

Consider the evolution of circular initial temperature profile in graphene [74]. Corresponding temperature field at $t = 20\tau_e$ is shown in Fig. 24.12. The figure shows, in particular, that the heat front is a circle as predicted by the derived formulae and the Huygens principle. At the same time, the temperature field has a symmetry of

the lattice, i.e., the heat transport is *strongly anisotropic*. Moreover, the temperature field has contributions from acoustic and optical branches of the dispersion relation. Acoustic waves have larger group velocities than optical waves; therefore, the temperature front on the left-hand side propagates faster than that on the right-hand side. We note that the temperature has a local minimum at the center. Therefore, the heat flows from "cold" to "hot".

24.4.3 The Influence of Nonlinearity

We conclude this section by investigating the effect of anharmonicity on heat transfer. As an example, we consider equilibration of a sinusoidal modulation of temperature in the β–Fermi–Pasta–Ulam–Tsingou (FPUT) chain [57]. In this system, the particles are connected to their nearest neighbors by the potential, which includes the quadratic term with the harmonic constant C and the quartic term with the anharmonic constant β.

The results for different values of the anharmonicity parameter β and for different wavelengths of temperature modulation were obtained numerically and compared to the analytical solution available for the linear case, i.e., $\beta = 0$ (see formula 24.30). Also, the applicability of the linear theory to a weakly nonlinear chain was assessed for different wavelengths of temperature modulation. The initial conditions of two types were used: (i) at $t = 0$, the energy of the system is in the form of kinetic energy with zero potential energy and (ii) the other major part of the energy is initially shared between kinetic and potential energies.

Firstly, for the linear chain ($\beta = 0$), the numerical results averaged over an increasing number of realizations converged to the analytical solution. This solution predicts that equilibration of a sinusoidal modulation of temperature demonstrates oscillations with a decrease in time amplitude, following the Bessel function of the first kind. This was true for the initial conditions of both types, though convergence with an increasing number of realizations was faster for the initial conditions with nearly equal kinetic and potential energies. Convergence was also faster for a larger wavelength of temperature modulation. The kinetics of temperature equilibration, for increasing number of realizations, converges not only for the harmonic chain but also for $\beta > 0$.

Secondly, with an increase in the degree of anharmonicity, the oscillatory equilibration of temperature gradually transforms into a monotonic one. For a given temperature wavelength modulation, there exists a value of the anharmonicity parameter when the temperature equilibration occurs most rapidly. For smaller values of β, oscillations of temperature decay slowly, and for larger β, the monotonic decay is slow (see Fig. 24.13).

Thirdly, the linear theory remains informative for weakly anharmonic chains when β is smaller than a certain critical value, which decreases with increasing temperature modulation wavelength. This means that temperature modulation with short wavelength is less affected by the anharmonicity or, in other words, the linear theory

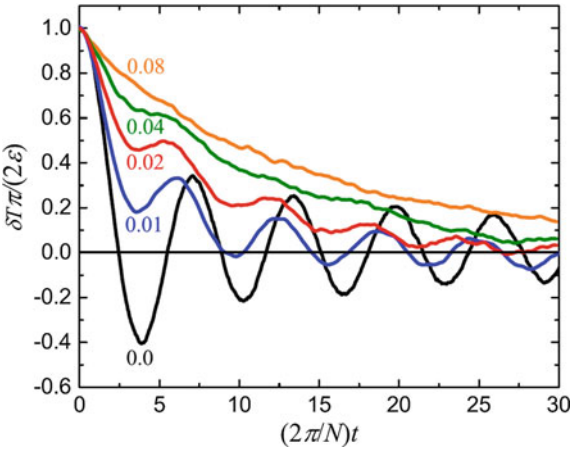

Fig. 24.13 Normalized difference between the averaged temperatures of the left and right halves of the chain, δT, as a function of normalized time for different values of the nonlinearity parameter β; the chain consists of $N = 32768$ particles [57]

remains valid for larger values of β, as compared to the long-wavelength temperature modulation.

Overall, these results have confirmed that (i) the continuum equation derived in [61] accurately describes the temperature flow in linear chains, (ii) linear theory remains informative for weakly anharmonic chains, and (iii) short-wavelength modulations of temperature are less affected by the anharmonicity and linear theory remains valid for larger values of β, as compared to the long-wavelength modulations of temperature.

In this regard, the results presented in previous works, e.g., [27] have found their explanation. Oscillations of the short-wavelength sinusoidal temperature modulation, observed by the authors of those works, can be well explained by the linear theory [61]. The oscillations were not observed by the authors for long-wavelength temperature modulation because, in this case, the effect of anharmonicity is much stronger. The oscillations of long-wavelength temperature modulation can be observed for smaller values of the anharmonicity parameter.

24.5 Thermoelasticity: Ballistic Resonance in FPUT Chain

The previous sections dealt mostly with crystalline solids with linear interactions between the particles. The considered linear models allow an analytical description of elasticity, transient thermal processes, and heat energy transfer (thermal conduction) in crystalline solids. However, they are unsuitable for describing thermoelastic effects such as thermal expansion or the conversion of mechanical energy into thermal energy. In this section, we address some effects caused by nonlinearity of interatomic interaction.

In [63] one-dimensional chains with pair force interactions are considered. Using the approach proposed in [59], the continualization of the dynamics and energy balance equations is carried out. As a result, the coupled thermoelasticity equations for a chain are obtained. As an example, we consider the well-known α–Fermi–Pasta–Ulam–Tsingou (FPUT) model [21], a one-dimensional chain with quadratic nonlinearity. All of the aforementioned thermomechanical processes can be qualitatively described by this model. Despite the apparent simplicity of the model, the analytical description of the macroscopic thermoelastic processes, thermal conductivity, and the transition of mechanical energy into thermal energy seems to be a very difficult and yet unsolved problem. The FPUT chain demonstrates anomalous thermomechanical properties. It is shown in [16, 17, 27, 117] that the heat conduction in the FPUT chain is represented neither by the Fourier law nor by the Maxwell–Cattaneo equation. In the limiting case of large times and infinitely long chain, the heat conduction is described by the equation with fractional derivatives [89]. However, this model does not capture the quasi-ballistic heat transfer typical for small times and chains of finite length. Therefore, the results obtained in Sect. 24.4 are used to describe the quasi-ballistic heat conduction regime.

An even more complicated problem is the description of the transition of mechanical energy into thermal energy. This process is in charge, in particular, of the damping of macroscopic mechanical vibrations of the chain. The study of the decay of mechanical vibrations of the FPUT chain has a long history, beginning with the pioneering work of Fermi, Past, and Ulam [21]. In [21], the initial conditions corresponding to the excitation of the first eigenmode of the chain were considered. It was shown numerically that the oscillations damping occurs non-monotonically: the decay and growth of the energy of mechanical oscillations alternate. In the literature, this effect is often referred to as *Fermi–Pasta–Ulam–Tsingou recurrence paradox* (see, for example, [22] for the review of the works aimed at explaining this paradox). Note that in the formulation proposed in the original paper [21], the oscillations were considered at zero initial temperature. In what follows, it is shown that the introduction of a finite temperature (random particle velocities) allows us to provide a monotonic damping of mechanical energy [76].

In this section, we describe thermomechanical phenomena observed in the α–FPUT chain with a spatially sinusoidal profile of initial temperature [76]. Firstly, it is shown analytically that temperature oscillations, caused by quasiballistic heat transport, and thermal expansion give rise to mechanical vibrations with growing amplitude. This new phenomenon is referred to as *ballistic resonance* [76]. Secondly, it is demonstrated numerically that mechanical vibrations, excited by the ballistic resonance, decay monotonically in time. Therefore at finite temperatures the FPUT recurrence paradox is eliminated.

Consider the equations of motion of $\alpha-$FPUT chain under periodic boundary conditions

$$m\ddot{u}_n = C(u_{n+1} - 2u_n + u_{n-1}) + \alpha\left((u_{n+1} - u_n)^2 - (u_n - u_{n-1})^2\right), \qquad (24.34)$$

where the parameter α characterizes nonlinearity. We consider initial conditions, corresponding to spatially sinusoidal kinetic temperature profile, zero initial fluxes, and no macroscopic mechanical motions

$$u_n = 0, \quad \dot{u}_n = \sigma_n \sqrt{\frac{2k_B}{m}\left(T_b + \Delta T \sin\frac{2\pi n}{N}\right)}, \qquad \langle\sigma_n\rangle = 0, \qquad \langle\sigma_n^2\rangle = 1, \tag{24.35}$$

where σ_n are uncorrelated random numbers with zero mean and unit variance; T_b is the average (background) temperature; ΔT is an amplitude of the initial temperature profile.

Next, we separate the motions [63]. Mechanical motion is associated with the time evolution of the mathematical expectation of particle displacement, whereas the thermal motion is defined as the difference between the total displacement and the mechanical one. Note that, in contrast to mechanical displacements, the thermal displacements are random.

We assume that the macroscopic mechanical motion of the chain is described by the equation of linear thermoelasticity, as shown in [63], while the behavior of temperature (heat transfer) is described by the ballistic heat Eq. (24.11) [61, 64]. Conversion of mechanical energy to thermal energy is neglected, then the macroscopic behavior of the chain in the continuum limit is described by the system of equations

$$\ddot{u} = c_S^2\left(u'' - \beta T'\right), \quad \ddot{T} + \frac{1}{t}\dot{T} = c_S^2 T'', \tag{24.36}$$

where c_S is the speed of sound and β is the thermal expansion coefficient. Note that both macroscopic equations are derived from the equations of motion (24.34). Anharmonic effects are taken into account only in the equation for the displacements, whereas the second one is derived using harmonic approximation, therefore it corresponds to the purely ballistic heat transport regime.

Substituting the solution of the ballistic heat equation with initial conditions, corresponding to *sinusoidal* initial perturbation [61], into the dynamics Eq. (24.36), we obtain

$$\ddot{u} = c_S^2 u'' - \lambda c_S^2 \beta \Delta T J_0(\omega t)\cos\lambda x, \tag{24.37}$$

where $\lambda = 2\pi/L$, L is the the chain length, $\omega = \lambda c_S$.

It can be seen that the temperature acts as an external force, exciting the first normal mode of mechanical vibrations. From the properties of Bessel function it follows that the external force oscillates with frequency ω and decays as $1/\sqrt{t}$. Note that the frequency coincides with the first eigenfrequency of mechanical vibrations.

The solution of (24.37) yields an exact expression for displacements

$$u(x,t) = z(t)\cos\lambda x, \qquad z(t) = -\frac{\beta\Delta T\omega t}{\lambda} J_1(\omega t). \tag{24.38}$$

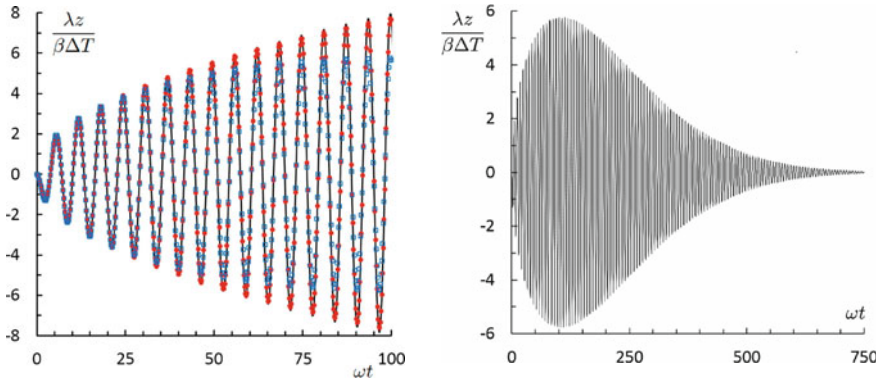

Fig. 24.14 **a** Growth of mechanical vibrations amplitude due to ballistic resonance: analytical solution (solid line) and numerical results for $\alpha a/C = -0.25$ (circles) and $\alpha a/C = -1$ (squares); **b** decay of mechanical vibrations amplitude for large times (numerical results, $\alpha a/C = -1$) [76]

At large times, the amplitude of displacement grows as a square root of time

$$z(t) \simeq -\sqrt{\frac{2}{\pi}}\frac{\beta \Delta T}{\lambda}\sqrt{\omega t}\cos\left(\omega t - \frac{3\pi}{4}\right). \tag{24.39}$$

The time dependence of the amplitude of mechanical vibrations $z(t)$ is presented in Fig. 24.14a. It can be seen that the amplitude grows in time, as described by the analytical solution (24.38). Thus the coincidence of a frequency of temperature oscillations with the first eigenfrequency of the chain leads to excitation of mechanical vibrations with growing amplitude. This phenomenon is referred to as *ballistic resonance* [76]. Note that, in contrast to the conventional mechanical resonance, the ballistic resonance occurs in the closed system without any external excitation. It is caused by conversion of thermal energy to mechanical energy.

Numerical simulations show that mechanical vibrations, excited by the ballistic resonance, decay in time (see Fig. 24.14b). The decay is caused by thermalization, i.e., conversion of mechanical energy to thermal energy. This process is not covered by our continuum model (24.36). The simulation results show that the mechanical oscillations arising at resonance decay monotonically. Therefore, the classical FPUT paradox is not observed at the finite temperature. In our calculations, the mechanical energy of the system is significantly lower than the thermal energy. It seems that this condition is necessary for monotonic decay. However, a rigorous proof of this statement requires further investigations.

24.6 Concluding Remarks

This paper summarizes the current status of research on discrete thermomechanics carried out in the Institute for Problems in Mechanical Engineering of the Russian Academy of Sciences. The main achievement is an approach for the analytical description of unsteady thermomechanical processes in perfect crystals in continuum approximation. The approach allows to describe the transition to thermal equilibrium, ballistic heat transfer, heat supply, propagation of thermoelastic waves, and other non-equilibrium processes in perfect crystals. One, two, and three-dimensional perfect crystals with arbitrary harmonic and weakly anharmonic interactions are considered. The approach predicts the existence of many peculiar thermomechanical phenomena, including but not limited to thermal waves, heat flow from cold to hot, several kinetic temperatures, thermal echo, and ballistic resonance. Still, we believe that many phenomena are yet to be discovered.

However, despite the significant progress in describing and understanding thermomechanical processes, many questions remain open. Let us briefly mention some aspects of the approach that require additional investigation.

- The relation between the kinetic temperature, defined above, and other definitions of temperature available in the literature is not straightforward. Which of these temperatures is the best parameter for the description of the thermal state of a non-equilibrium system? This question requires a separate discussion.
- Some of the presented results (e.g., heat flowing from cold to hot) seem to contradict the second law of thermodynamics. We refer to papers [62, 112] for further discussion of this important issue.
- Many of the results have been obtained for one particular type of initial conditions, namely random initial velocities and zero displacements. These initial conditions are the simplest model of a heat impact on a system. How well does this model describe the crystal heating, e.g., by a short laser pulse?
- The results have been mostly obtained in the harmonic approximation. What is the range of applicability of this approximation for real materials? To what extent can quantum effects be ignored inside this range?
- Kinetic theory is a powerful tool for the description of the thermomechanical processes in discrete systems. In some cases, the kinetic approach can be derived from the dynamical description [77]. However, in general, the establishment of this link is still connected with a number of open questions.

We are planning to address these fundamental questions in our future work.

Acknowledgements The authors acknowledge the financial support of this work by the Russian Foundation for Basic Research (A.M. Krivtsov, project No.19-01-00633; V.A. Kuzkin and E.A. Podolskaya, project No.20-37-70058).

References

1. Abramyan, A.K., Bessonov, N.M., Mirantsev, L.V., Reinberg, N.A.: Influence of liquid environment and bounding wall structure on fluid flow through carbon nanotubes. Phys. Lett. A **379**, 1274–1282 (2015)
2. Allen, M.P., Tildesley, D.J.: Computer Simulation of Liquids. Clarendon Press, Oxford (1987)
3. Anisimov, S.I., Zhakhovskii, V.V., Fortov, V.E.: Shock wave structure in simple liquids. JETP Lett. **65**(9), 722–727 (1997)
4. Ashcroft, N., Mermin, N.: Solid State Physics. Saunders College Publishing, Philadelphia (1976)
5. Babenkov, M.B., Krivtsov, A.M., Tsvetkov, D.V.: Energy oscillations in 1D harmonic crystal on elastic foundation. Phys. Mesomech. **19**(1), 60–67 (2016)
6. Balandin, A.A.: Thermal properties of graphene and nanostructured carbon materials. Nat. Mater. **10**, 569–581 (2011)
7. Barani, E., Lobzenko, I.P., Korznikova, E.A., Soboleva, E.G., Dmitriev, S.V., Zhou, K., Marjaneh, A.M.: Transverse discrete breathers in unstrained graphene. Eur. Phys. J. B **90**(3), 1–5 (2017)
8. Berinskii, I.E., Kuzkin, V.A.: Equilibration of energies in a two-dimensional harmonic graphene lattice. Philos. Trans. R. Soc. A **378**(2162), 20190114 (2020)
9. Bhatnagar, P.L., Gross, E.P., Krook, M.: A model for collision processes in gases. I. Small amplitude processes in charged and neutral one-component systems. Phys. Rev. **94**(3), 511–525 (1954)
10. Boldrighini, C., Pellegrinotti, A., Triolo, L.: Convergence to stationary states for infinite harmonic systems. J. Stat. Phys. **30**(1), 123–155 (1983)
11. Casas-Vazquez, J., Jou, D.: Temperature in non-equilibrium states: a review of open problems and current proposals. Rep. Prog. Phys. **66**, 1937–2023 (2003)
12. Casher, A., Lebowitz, J.L.: Heat flow in regular and disordered harmonic chains. J. Math. Phys. **12**, 1701–1711 (1971)
13. Chandrasekharaiah, D.S.: Hyperbolic thermoelasticity: a review of recent literature. Appl. Mech. Rev. **39**, 355–376 (1986)
14. Chang, C.W., Okawa, D., Garcia, H., Majumdar, A., Zettl, A.: Breakdown of Fouriers law in nanotube thermal conductors. Phys. Rev. Lett. **101**, 075903 (2008)
15. Chen, G.: Ballistic-diffusive heat conduction equations. Phys. Rev. Lett. **85**, 2297–2300 (2001)
16. Das, S.G., Dhar, A., Narayan, O.: Heat conduction in the $\alpha - \beta$ Fermi-Pasta-Ulam chain. J. Stat. Phys. **154**(1–2), 204–213 (2014)
17. Das, S.G., Dhar, A., Saito, K., Mendl, C.B., Spohn, H.: Numerical test of hydrodynamic fluctuation theory in the Fermi-Pasta-Ulam chain. Phys. Rev. E **90**(1), 012124 (2014)
18. Dhar, A.: Heat transport in low-dimensional systems. Adv. Phys. **57**, 457–537 (2008)
19. Dhar, A., Saito, K.: Heat Transport in Harmonic Systems. In: Lepri, S. (ed.) Thermal transport in low dimensions. Lecture Notes in Physics **921**, 305–338 (2016)
20. Dudnikova, T.V., Komech, A.I., Spohn, H.: On the convergence to statistical equilibrium for harmonic crystals. J. Math. Phys. **44**, 2596–2620 (2003)
21. Fermi, E., Pasta, J., Ulam, S.: Studies of nonlinear problems. Document LA 1940. Los Alamos National Laboratory (1955)
22. The Fermi-Pasta-Ulam problem: a status report. In: Gallavotti, G. (ed.) Lecture Notes in Physics, vol. 728 (2008)
23. Gavrilov, S.N., Krivtsov, A.M.: Thermal equilibration in a one-dimensional damped harmonic crystal. Phys. Rev. E **100**, 022117 (2019)
24. Gavrilov, S.N., Krivtsov, A.M., Tsvetkov, D.V.: Heat transfer in a one-dimensional harmonic crystal in a viscous environment subjected to an external heat supply. Contin. Mech. Thermodyn. **31**(1), 255–272 (2019)
25. Gavrilov, S.N., Krivtsov, A.M.: Steady-state kinetic temperature distribution in a two-dimensional square harmonic scalar lattice lying in a viscous environment and subjected to a point heat source. Contin. Mech. Thermodyn. **32**(1), 41–61 (2020)

26. Gendelman, O.V., Savin, A.V.: Normal heat conductivity of the one-dimensional lattice with periodic potential of nearest-neighbor interaction. Phys. Rev. Lett. **84**(11), 2381–2384 (2000)
27. Gendelman, O.V., Savin, A.V.: Nonstationary heat conduction in one-dimensional chains with conserved momentum. Phys. Rev. E **81**, 020103 (2010)
28. Goldstein, R.V., Morozov, N.F.: Mechanics of deformation and fracture of nanomaterials and nanotechnology. Phys. Mesomech. **10**(5–6), 235–246 (2007)
29. Golovnev, I.F., Golovneva, E.I., Konev, A.A., Fomin, V.M.: Physical mesomechanics and molecular dynamic modeling. Phys. Mesomech. **1**(2), 19 (1998)
30. Golovneva, E.I., Golovnev, I.F., Fomin, V.M.: Simulation of quasistatic processes in crystals by a molecular dynamics method. Phys. Mesomech. **6**(5–6), 41–46 (2003)
31. Guo, P., Gong, J., Sadasivam, S., Xia, Y., Song, T.-B., Diroll, B.T., Stoumpos, C.C., Ketterson, J.B., Kanatzidis, M.G., Chan, M.K.Y., Darancet, P., Xu, T., Schaller, R.D.: Slow thermal equilibration in methylammonium lead iodide revealed by transient mid-infrared spectroscopy. Nat. Commun. **9**, 2792 (2018)
32. Guzev, M.A.: The exact formula for the temperature of a one-dimensional crystal. Dalnevost. Mat. Zh. **18**, 39–47 (2018)
33. Harris, L., Lukkarinen, J., Teufel, S., Theil, F.: Energy transport by acoustic modes of harmonic lattices. SIAM J. Math. Anal. **40**(4), 1392–1418 (2008)
34. Hemmer, P.C.: Dynamic and stochastic types of motion in the linear chain. Norges Tekniske Hoiskole (1959)
35. Holian, B.L., Hoover, W.G., Moran, B., Straub, G.K.: Shock-wave structure via nonequilibrium molecular dynamics and Navier–Stokes continuum mechanics. Phys. Rev. A **22**, 2798 (1980)
36. Holian, B.L., Mareschal, M.: Heat-flow equation motivated by the ideal-gas shock wave. Phys. Rev. E **82**, 026707 (2010)
37. Hoover, W.G., Hoover, C.G., Travis, K.P.: Shock-wave compression and Joule–Thomson expansion. Phys. Rev. Lett. **112**, 144504 (2014)
38. Hoover, W.G.: Computational statistical mechanics. Studies in modern thermodynamics. Elsevier Science (1991)
39. Hsiao, T.K., Chang, H.K., Liou, S.-C., Chu, M.-W., Lee, S.-C., Chang, C.-W.: Observation of room-temperature ballistic thermal conduction persisting over 8.3 μm SiGe nanowires. Nat. Nanotechnol. **8**(7), 534–538 (2013)
40. Hua, C., Minnich, A.J.: Transport regimes in quasiballistic heat conduction. Phys. Rev. B **89**, 094302 (2014)
41. Huberman, S., Duncan, R.A., Chen, K., Song, B., Chiloyan, V., Ding, Z., Maznev, A.A., Chen, G., Nelson, K.A.: Observation of second sound in graphite at temperatures above 100 K. Science **364**(6438), 375–379 (2019)
42. Huerta, M.A., Robertson, M.A.: Exact equilibration of harmonically bound oscillator chains. J. Math. Phys. **12**, 2305–2311 (1971)
43. Indeitsev, D.A., Naumov, V.N., Semenov, B.N., Belyaev, A.K.: Thermoelastic waves in a continuum with complex structure. ZAMM **89**, 279–287 (2009)
44. Indeitsev, D.A., Osipova, E.V.: A two-temperature model of optical excitation of acousticwaves in conductors. Dokl. Phys. **62**(3), 136–140 (2017)
45. Inogamov, N.A., Petrov, Yu.V., Zhakhovsky, V.V., Khokhlov, V.A., Demaske, B.J., Ashitkov, S.I., Khishchenko, K.V., Migdal, K.P., Agranat, M.B., Anisimov, S.I., Fortov, V.E., Oleynik, I.I.: Two-temperature thermodynamic and kinetic properties of transition metals irradiated by femtosecond lasers. AIP Conf. Proc. **1464**(1), 593–608 (2012)
46. Ivanova, E.A., Krivtsov, A.M., Morozov, N.F.: Bending stiffness calculation for nanosize structures. Fatigue Fract. Eng. Mater. Struct. **26**, 715–718 (2003)
47. Ivanova, E.A., Krivtsov, A.M., Morozov, N.F., Firsova, A.D.: Description of crystal packing of particles with torque interaction. Mech. Solids **38**(4), 76–88 (2003)
48. Ivanova, E.A.: On a micropolar continuum approach to some problems of thermo- and electrodynamics. Acta Mech. **230**(5), 1685–1715 (2019)

49. Johnson, J.A., Maznev, A.A., Cuffe, J., Eliason, J.K., Minnich, A.J., Kehoe, T., Sotomayor Torres, C.M., Chen, G., Nelson, K.A.: Direct measurement of room-temperature nondiffusive thermal transport over micron distances in a silicon membrane. Phys. Rev. Lett. **110**, 025901 (2013)
50. Kannan, V., Dhar, A., Lebowitz, J.L.: Nonequilibrium stationary state of a harmonic crystal with alternating masses. Phys. Rev. E **85**, 041118 (2012)
51. Kato, A., Jou, D.: Breaking of equipartition in one-dimensional heat-conducting systems. Phys. Rev. E **64**, 052201 (2001)
52. Klein, G.: Prigogine, I: Sur la mecanique statistique des phenomenes irreversibles III. Physica **19**, 1053 (1953)
53. Klemens, P.G.: The thermal conductivity of dielectric solids at low temperatures. Proc. R. Soc. A **208**(1092), 108–133 (1951)
54. Koh, Y.K., Cahill, D.G., Sun, B.: Nonlocal theory for heat transport at high frequencies. Phys. Rev. B **90**(20), 205412 (2014)
55. Korikov, D.V.: Asymptotic description of fast thermal processes in scalar harmonic lattices. Phys. Solid State **62**(11), 2232–2241 (2020)
56. Korobeynikov, S.N.: Nonlinear equations of deformation of atomic lattices. Arch. Mech. **57**(6), 435–453 (2005)
57. Korznikova, E.A., Kuzkin, V.A., Krivtsov, A.M., Xiong, D., Gani, V.A., Kudreyko, A.A., Dmitriev, S.V.: Equilibration of sinusoidal modulation of temperature in linear and nonlinear chains. Phys. Rev. E **102**(4), 062148(6) (2020)
58. Kosevich, Y.A., Savin, A.V.: Confining interparticle potential makes both heat transport and energy diffusion anomalous in one-dimensional phononic systems. Phys. Lett. A **380**, 3480–3484 (2016)
59. Krivtsov, A.M.: Deformation and Fracture of Solids with Microstructure. Fizmatlit, Moscow (2007).[in Russian]
60. Krivtsov, A.M.: Energy oscillations in a one-dimensional crystal. Dokl. Phys. **59**(9), 427–430 (2014)
61. Krivtsov, A.M.: Heat transfer in infinite harmonic one dimensional crystals. Dokl. Phys. **60**(9), 407–411 (2015)
62. Krivtsov, A.M., Sokolov, A.A., Müller, W.H., Freidin, A.B.: One-dimensional heat conduction and entropy production. Adv. Struct. Mater. **87**, 197–213 (2018)
63. Krivtsov, A.M., Kuzkin, V.A.: Discrete and continuum thermomechanics. In: Altenbach, H., Öchsner, A. (eds.) Encyclopedia of Continuum Mechanics. Springer, Berlin, Heidelberg (2018)
64. Krivtsov, A.M.: The ballistic heat equation for a one-dimensional harmonic crystal. In: Altenbach, H., Belyaev, A., Eremeyev, V.A., Krivtsov, A.M., Porubov, A.V. (eds.) Dynamical Processes in Generalized Continua and Structures. Springer, Berlin (2019)
65. Krivtsov, A.M., Podolskaya, E.A., Shubina, V.Y.: Asymptotics of a thermal wave in a one-dimensional harmonic crystal. Mater. Phys. Mech. **42**, 837–845 (2019)
66. Krivtsov, A.M., Babenkov, M.B., Tsvetkov, D.V.: Heat propagation in a one-dimensional harmonic crystal on an elastic foundation. Phys. Mesomech. **23**(2), 109–119 (2020)
67. Kuksin, AYu., Morozov, I.V., Norman, G.E., Stegailov, V.V., Valuev, I.A.: Standard of molecular dynamics modelling and simulation of relaxation. Mol. Simul. **31**, 1005–1017 (2005)
68. Kukushkin, S.A.: Evolution processes in multicomponent and multiphase films. Thin Solid Films **207**(1–2), 302–312 (1992)
69. Kukushkin, S.A., Osipov, A.V., Telyatnik, R.S.: Elastic interaction of point defects in cubic and hexagonal crystals. Phys. Solid State **58**(5), 971–980 (2016)
70. Kuzkin, V.A., Krivtsov, A.M.: High-frequency thermal processes in harmonic crystals. Dokl. Phys. **62**(2), 85–89 (2017)
71. Kuzkin, V.A., Krivtsov, A.M.: An analytical description of transient thermal processes in harmonic crystals. Phys. Solid State **59**(5), 1051–1062 (2017)
72. Kuzkin, V.A., Krivtsov, A.M.: Fast and slow thermal processes in harmonic scalar lattices. J. Phys.: Condens. Matter **29**, 505401 (2017)

73. Kuzkin, V.A.: Thermal equilibration in infinite harmonic crystals. Contin. Mech. Thermodyn. **31**, 1401–1423 (2019)
74. Kuzkin, V.A.: Unsteady ballistic heat transport in harmonic crystals with polyatomic unit cell. Contin. Mech. Thermodyn. **31**(6), 1573–1599 (2019)
75. Kuzkin, V.A., Liazhkov, S.D.: Equilibration of kinetic temperatures in face-centered cubic lattices. Phys. Rev. E **102**(4), 042219 (2020)
76. Kuzkin, V.A., Krivtsov, A.M.: Ballistic resonance and thermalization in the Fermi-Pasta-Ulam-Tsingou chain at finite temperature. Phys. Rev. E **101**, 042209 (2020)
77. Kuzkin, V.A., Krivtsov, A.M.: Unsteady ballistic heat transport: linking lattice dynamics and kinetic theory. Acta Mech. **232**(5), 1983–1996 (2021)
78. Lanford, O.E., Lebowitz, J.L.: Time evolution and ergodic properties of harmonic systems. In: Moser, J. (ed.) Dynamical Systems, Theory and Applications. Lecture Notes in Physics, vol. 38. Springer, Berlin, Heidelberg (1975)
79. Le-Zakharov, A.A., Krivtsov, A.M.: Molecular dynamics investigation of heat conduction in crystals with defects. Dokl. Phys. **53**(5), 261–264 (2008)
80. Le-Zakharov, A.A., Krivtsov, A.M., Porubov, A.V.: Relation between defects and crystalline thermal conduction. Contin. Mech. Thermodyn. **31**(6), 1873–1881 (2019)
81. Lepri, S., Livi, R., Politi, A.: Thermal conduction in classical low-dimensional lattices. Phys. Rep. **377**, 1–80 (2003)
82. Lepri, S., Mejia-Monasterio, C., Politi, A.: A stochastic model of anomalous heat transport: analytical solution of the steady state. J. Phys. A **42**(2), 025001 (2008)
83. Lepri, S., Mejia-Monasterio, C., Politi, A.: Nonequilibrium dynamics of a stochastic model of anomalous heat transport. J. Phys. A **43**, 065002 (2010)
84. Linn, S.L., Robertson, H.S.: Thermal energy transport in harmonic systems. J. Phys. Chem. Solids **45**(2), 133–140 (1984)
85. Loboda, O.S., Krivtsov, A.M., Porubov, A.V., Tsvetkov, D.V.: Thermal processes in a one-dimensional crystal with regard for the second coordination sphere. ZAMM **99**(9), e201900008 (2019)
86. Loboda, O.S., Podolskaya, E.A., Tsvetkov, D.V., Krivtsov, A.M.: On the fundamental solution of the heat transfer problem in one-dimensional harmonic crystals. Contin. Mech. Thermodyn. **33**(2), 485–496 (2021)
87. Lomakin, E.V., Lurie, S.A., Belov, P.A., Rabinskiy, L.N.: On the generalized heat conduction laws in the reversible thermodynamics of a continuous medium. Dokl. Phys. **63**(12), 503–507 (2018)
88. Lurie, S.A., Belov, P.A.: On the nature of the relaxation time, the Maxwell–Cattaneo and Fourier law in the thermodynamics of a continuous medium, and the scale effects in thermal conductivity. Contin. Mech. Thermodyn. **32**, 709–728 (2018)
89. Mellet, A., Merino-Aceituno, S.: Anomalous energy transport in FPU$-\beta$ chain. J. Stat. Phys. **160**, 583–621 (2015)
90. Mielke, A.: Macroscopic behavior of microscopic oscillations in harmonic lattices via Wigner-Husimi transforms. Arch. Ration. Mech. Anal. **181**, 401–448 (2006)
91. Murachev, A.S., Krivtsov, A.M., Tsvetkov, D.V.: Thermal echo in a finite one-dimensional harmonic crystal. J. Phys.: Condens. Matter **31**(9), 095702 (2019)
92. Muratikov, K.L.: Theory of the generation of mechanical vibrations by laser radiation in solids containing internal stresses on the basis of the thermoelastic effect. Tech. Phys. **44**, 792–796 (1999)
93. Norman, G.E., Stegailov, V.V.: Stochastic theory of the classical molecular dynamics method. Math. Models Comput. Simul. **5**, 305–333 (2013)
94. Peierls, R.: Zur kinetischen theorie der warmeleitung in kristallen. Ann. Phys. **3**, 1055 (1929)
95. Piazza, F., Lepri, S.: Heat wave propagation in a nonlinear chain. Phys. Rev. B **79**, 094306 (2009)
96. Podolskaya, E.A., Krivtsov, A.M., Tsvetkov, D.V.: Anomalous heat transfer in one-dimensional diatomic harmonic crystal. Mater. Phys. Mech. **40**, 172–180 (2018)

97. Porubov, A.V., Belyaev, A.K., Polyanskiy, V.A.: Nonlinear hybrid continuum-discrete dynamic model of influence of hydrogen concentration on strength of materials. Contin. Mech. Thermodyn. **33**(4), 933–941 (2021)
98. Prigogine, I., Henin, F.: On the general theory of the approach to equilibrium. I: interacting normal modes. J. Math. Phys. **1**(5), 349–371 (1960)
99. Psakhie, S.G., Ostermeyer, G.P., Dmitriev, A.I., Shilko, E.V., Smolin, A.Y., Korostelev, S.Y.: Method of movable cellular automata as a new trend of discrete computational mechanics. I: theoretical description. Phys. Mesomech. **3**(2), 5–12 (2000)
100. Rieder, Z., Lebowitz, J.L., Lieb, E.: Properties of a harmonic crystal in a stationary nonequilibrium state. J. Math. Phys. **8**, 1073–1078 (1967)
101. Rogers, J.A., Maznev, A.A., Banet, M.J., Nelson, K.A.: Optical generation and characterization of acousticwaves in thin films: fundamentals and applications. Annu. Rev. Mater. Sci. **30**, 117–157 (2000)
102. Romano, G., Grossman, J.C.: Heat conduction in nanostructured materials predicted by phonon bulk mean free path distribution. J. Heat Transf. **137**, 071302 (2015)
103. Saadatmand, D., Xiong, D., Kuzkin, V.A., Krivtsov, A.M., Savin, A.V., Dmitriev, S.V.: Discrete breathers assist energy transfer to AC driven nonlinear chains. Phys. Rev. E **97**, 022217 (2018)
104. Savin, A.V., Zolotarevskiy, V., Gendelman, O.V.: Normal heat conductivity in two-dimensional scalar lattices. EPL **113**, 24003 (2016)
105. Savin, A.V., Zolotarevskiy, V., Gendelman, O.V.: Heat conduction in diatomic chains with correlated disorder. Phys. Lett. A **381**(3), 145–152 (2017)
106. Schrödinger, E.: Zur dynamik elastisch gekoppelter punktsysteme. Ann. Phys. **44**, 916–934 (1914)
107. Sinha, S., Goodson, K.E.: Review: multiscale thermal modeling in nanoelectronics. Int. J. Multiscale Comput. Eng. **3**(1), 107–133 (2005)
108. Slepyan, L.I.: On the energy partition in oscillations and waves. Proc. R. Soc. A **471**, 20140838 (2015)
109. Spohn, H., Lebowitz, J.L.: Stationary non-equilibrium states of infinite harmonic systems. Commun. Math. Phys. **54**, 97 (1977)
110. Spohn, H.: The phonon Boltzmann equation, properties and link to weakly anharmonic lattice dynamics. J. Stat. Phys. **124**(2), 1041–1104 (2006)
111. Sokolov, A.A., Krivtsov, A.M., Müller, W.H.: Localized heat perturbation in harmonic 1D crystals: solutions for an equation of anomalous heat conduction. Phys. Mesomech. **20**(3), 305–310 (2017)
112. Sokolov, A.A., Krivtsov, A.M., Müller, W.H., Vilchevskaya, E.N.: Change of entropy for the one-dimensional ballistic heat equation: sinusoidal initial perturbation. Phys. Rev. E **99**(4), 042107 (2019)
113. Tsaplin, V.A., Kuzkin, V.A.: Temperature oscillations in harmonic triangular lattice with random initial velocities. Lett. Mater. **8**(1), 16–20 (2018)
114. Titulaer, U.M. Ergodic features of harmonic-oscillator systems. III: asymptotic dynamics of large systems. Physica **70**(3), 456–474 (1973)
115. Tzou, D.Y.: Macro- to microscale heat transfer: the lagging behavior. Wiley (2014)
116. Uribe, F.J., Velasco, R.M., Garcia-Colin, L.S.: Two kinetic temperature description for shock waves. Phys. Rev. E **58**, 3209–3222 (1998)
117. Xiong, D.: Heat perturbation spreading in the Fermi-Pasta-Ulam system with next-nearest-neighbor coupling: competition between phonon dispersion and nonlinearity. Phys. Rev. E **95**(6), 062140 (2017)
118. Xu, X., Pereira, L.F., Wang, Y., Wu, J., Zhang, K., Zhao, X., Bae, S., Bui, C.T., Xie, R., Thong, J.T., Hong, B.H., Loh, K.P., Donadio, D., Li, B., Ozyilmaz, B.: Length-dependent thermal conductivity in suspended single-layer graphene. Nat. Commun. **5**, 3689 (2014)
119. Ziman, J.M.: Electrons and Phonons. The theory of transport phenomena in solids, Oxford University Press, New York (1960)